

Research on Automatic Baggage and Cargo Handling System of Airport with Computer Artificial Intelligence

Haitao Liu, Hongxia Zhang

Weihai Guangtai Airport Equipment Co., Ltd, Weihai 264200, Shandong, PR China

Abstract

This paper designs the intelligent handling system of airport baggage. The system includes camera module, carrier frame, control core, drive module and power supply. CCD camera is used to collect images of underground wires to obtain the required data. An optimization method based on maximum and shortest completion period is proposed. The use of wireless communication technology, digital image processing and identification technology and bus technology to make the host and slave computer cooperate with each other, to achieve the purpose of collaborative work. Numerical experiments show that the method is effective.

Keywords

Airport; Artificial Intelligence; Handling System; Luggage; Mechanical Components; Machine Vision.

1. Introduction

At airports and other places, luggage is usually carried by manpower, which makes it inconvenient for the elderly and the sick to travel. If the luggage can be automatically followed, it can be a good solution to the inconvenience of luggage transportation. At present, automatic tracking technology still faces many problems, such as: the anti-interference ability of radio frequency identification positioning is weak, the deployment cost of ultra-wideband positioning is high, the basic requirements of the hardware equipment of ultrasonic positioning are high, and the anti-interference ability is weak. On this basis, a design method for motion robots based on multiple trajectories is proposed[1]. It also includes autonomous mobile robots such as unmanned trucks and AGVs, and airports are an important application site for handling robots. At present, many airports are using intelligent handling robots, such as in Shenzhen Airport, which uses the friction between the pallet area and the suitcase to move the luggage, but such a moving method is easy to cause the suitcase to slip from the pallet area, resulting in damage to personnel or the suitcase. The intelligent baggage sorting and handling robot used in Xiamen Airport uses the method of suction cup to load and unload baggage, but it is difficult to complete the loading and unloading work because of the insufficient adsorption capacity when the baggage is large. An automatic handling robot developed by Suzhou Bozhong Company can assist elderly and sick people in chairs to carry luggage to the departure hall, but it cannot complete tasks such as automatic identification and loading and unloading of luggage. Compared with the above loading and unloading robots, the intelligent loading and unloading system of airport baggage designed and researched in this paper can better solve the problem of "last kilometer". It can automatically adjust the spacing between two groups of friction plates and mechanical fingers according to the size of the package, so that it can grasp packages of various sizes [2]. And the extrusion and lifting methods used make the contact surface of the manipulator and the suitcase changed from the traditional 1 side to 3 sides, which greatly improves the reliability of the manipulator when it is assembled together to carry the package. The system consists of camera module, carrier frame, core control device, drive module and power supply device. CCD camera is

used to collect images of underground wires to obtain the required data. A mathematical programming model avoidance constraints is established.

2. Design of Automatic Handling System for Airport Baggage and Cargo

2.1 System Architecture

The system mainly consists of several main monitoring rooms and several slave transmission stations, and the data interaction between the two slave transmission stations is realized by wireless communication (Figure 1 quoted in COMSEC: Secure Communications for Baggage Handling Systems). The intelligent car owner system mainly includes: Transport image acquisition module, motor control module, steering control module, wireless communication module, and power management module. On the one hand, this system can capture the surrounding environment through the function of the camera, and on the other hand, it can feedback this information to the main monitoring station through wireless communication, so as to make accurate judgments on the vehicle's movement trajectory and speed. [3]. The intelligent vehicle wirelessly transmits its own coordinate information and image information to the main monitoring station, while the transportation system transmits the characteristics of the material itself obtained from the monitoring station to the company's management information system.

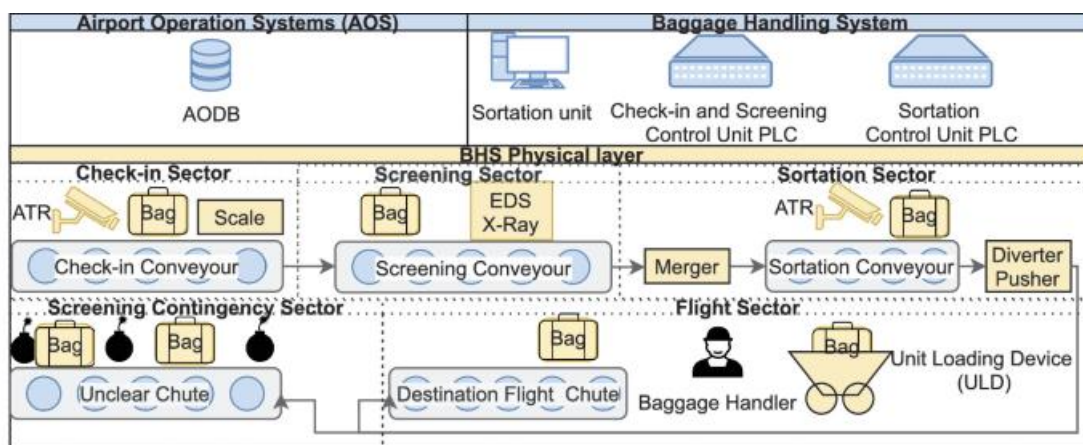


Figure 1. Architecture of automatic baggage handling system at airport

The controller of the intelligent vehicle uses Freescale's S12 series vehicle electronic control chip, and uses the high-speed A/D conversion device in the chip to collect and process the data of the CCD camera, so as to achieve the purpose of turning and driving speed for electric baggage handling. It realizes the effective control of wireless transmission, receiving and other functions, and realizes the wireless communication between the master station and the slave station [4]. After the work is sent from the master monitor to the slave station, the system initializes the modules, including the AD conversion module, PWM module, timer module, phase-locked loop module, and various I/O modules. After the end of initialization, the MCU uses the activated WEB to send and receive data, and analyzes the collected image data, and then combines it with the data sent by the received main monitoring system to adjust the direction and speed of the vehicle according to a specific decision rule. The collection of camera image data and the closed-loop adjustment of motor speed are realized by interrupt mode.

2.2 System Functions

2.2.1 Image Acquisition and Processing

The LM1881 of National Semiconductor is used to achieve simultaneous segmentation of multiple types of video data. The single chip computer can judge the starting time of each frame of the image and the starting time of each line of the image, so that the single chip computer can collect the image

signal with a certain sequential logic. The circuit diagram is shown in Figure 2. The image signal is connected via C1 to the second input pin of LM 1881, where pin 1 is line synchronous, pin 3 is field output, and pin 7 is parity field output. Image acquisition and image processing are the premise and basis visual navigation [5]. The single chip computer can accurately obtain the gray value of a 40.18 square image, which can well reflect the image information of the ground guide line. The central point method is used to obtain the deviation of the black line. These algorithms are filtered by using a boundary-based method to obtain the relative information of the reticle. During image processing, the output signal of the camera includes the voltage value corresponding to the gray level of the image, the blanking signal, the field synchronization signal, and the field blanking message. A line and a field synchronization signal separated from the microcontroller and the image signal are separated from the image and simultaneously driven by one or more images in the image, and collected into the image. The image acquisition and processing of the system are completed by calling the sub-function of image processing.

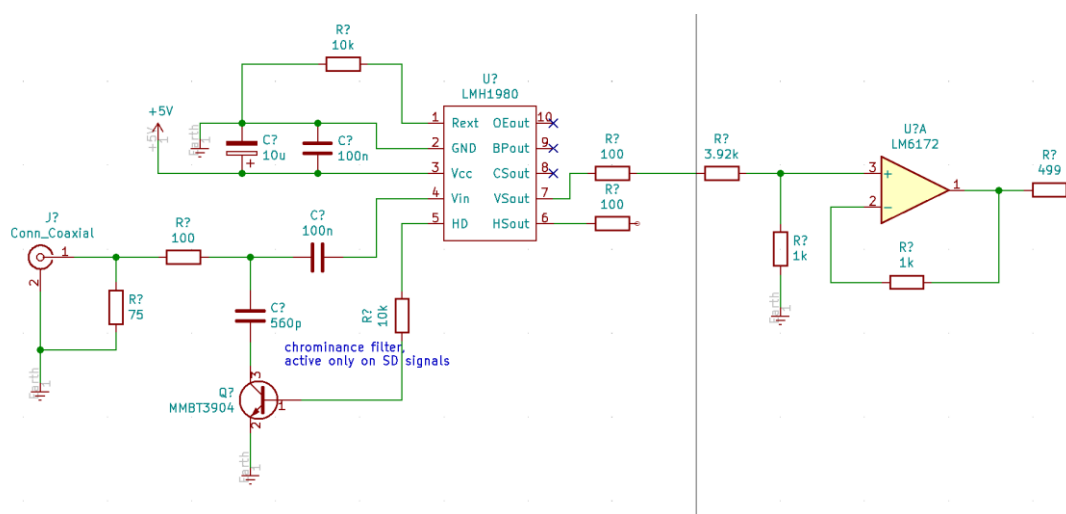


Figure 2. Circuit diagram of LM1881

2.2.2 System Communication Components

The MCU first transmits the configuration instructions to the communication module NRF905 through SPI, and then writes the configuration information in turn. This configuration information includes the operating frequency, transmission power, transmission and receive addresses, transmission and receive packet length and some modes of operation [6]. According to the requirements of the system, the wireless transmission and reception of data are completed. In the launching process of NRF905, the single-chip microcomputer will first set the TXEN end of the NRF905 module to a high position and the TRX_CE end to a low position, so that NRF905 is in the launching state. After that, the write to send address command WTA is sent through SPI, the address of the sent packet is written, and then the data is written through SPI. After the NRF905 is sent, the DR Bit will be set to a high position, and after the MCU detects that the DR Has become a high potential, the transmission program will end. In the receiving process of NRF905, when the data is received smoothly, the DR Will be placed at the high level. When the MCU detects that the DR Is changed at the high level, it will use SPI communication to write and read the data command RRP to NRF905, read the received data packet with SPI cycle, and store the data into the array. The receiving program ends when all data is received.

3. System Algorithm Design

3.1 Stereo Matching

In a dual CCD camera, two cameras on the left and right generate two images respectively, but for the same object, there is a certain degree of overlap in the view area of the two cameras on the left

and right. How to achieve the exact matching of the mapping relationship between the two cameras on the right and right by constructing the geometric restriction relationship of overlapping pixels is a problem [7]. This project plans to divide the three-dimensional space into two categories, one is the global matching algorithm, the other is the local matching algorithm. based on deviation minimization is adopted in this paper.

In the pixels of the cross region, the traversal field should be determined according to a given scale, such as 3×3 domain, 5×5 domain, so that the range used will become smaller, and the time required will become shorter. In the determined domain, when the cumulative deviation reaches the minimum value with the pixel of the corresponding domain of another image along the same line, it is considered that the optimal solution of local matching is found. The basic principles of this method, which has a minimum cumulative error, are:

$$\min_{s=s_{\min}}^{s_{\max}} \left(\sum_{i=-n/2}^{n/2} \left(\sum_{j=-n/2}^{n/2} \left| R_{right} [u+i][u+j] - R_{left} [u+i+s] \cdot [u+j] \right| \right) \right) \quad (1)$$

s_{\min} and s_{\max} are the minimum and maximum parallax, respectively. n is the size of the square neighborhood. R_{left}, R_{right} is the left image and the right image of the binocular CCD camera respectively. u, v are the image.

3.2 Binocular Ranging Principle

Binocular measurement is used to calculate the depth information of target object according to the mathematical principle of triangle based on camera calibration. As shown in Figure 3, the two lenses of the camera, whose optical axis is parallel along the w direction, have the same focal length, thus achieving the measurement of the viewing space [8]. The left and right cameras can obtain the image of the same object in the same scene, and the same feature points have two different positions in the left and right image plane, and the coordinate difference between them is parallax.

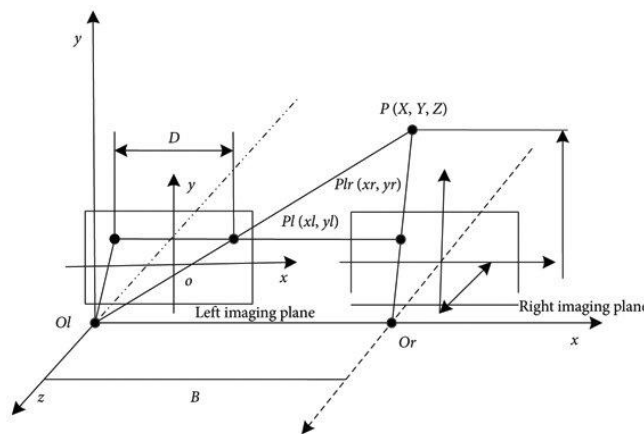


Figure 3. Principle of binocular vision ranging

The two lenses of the binocular CCD camera obtain the left and right images of the same feature point $Q(u_{\sigma}, v_{\sigma}, w_{\sigma})$ of the object, and their image coordinates are respectively recorded as $q_1(u_1, v_1), q_{\sigma}(u_{\sigma}, v_{\sigma})$. If the images of binocular CCD cameras are on the same plane, then the v coordinate of the image of feature point Q is the same, that is, $V_1 = V_{\sigma} = V$, then it is obtained by triangle similarity:

$$s = U_1 - U_\sigma \tag{2}$$

$$\frac{E}{w_\sigma} = \frac{E - (U_1 - U_\sigma)}{w_\sigma - g} = \frac{U_1 - U_\sigma}{g} = \frac{s}{g} \tag{3}$$

Formula (4) is the parallax of the left and right images. g is the focal length of the camera. E is the baseline distance, that is, the distance between the projection centers of the two lenses. Set the image coordinate $\alpha = U_1, \beta = V$, and the three-dimensional coordinate of the space point can be obtained from formula (3):

$$\frac{g}{w_\sigma} = \frac{\alpha}{u_\sigma} = \frac{\beta}{v_\sigma} \tag{4}$$

$$\begin{cases} u_\sigma = \alpha \frac{E}{s} \\ v_\sigma = \beta \frac{E}{s} \\ w_\sigma = g \frac{E}{s} \end{cases} \tag{5}$$

The 3D coordinates of each feature point on the whole image plane are obtained by iterative calculation of the feature cameras and stored as depth image data.

3.3 Determination of the Coordinates of the Target

In order to enable the robot arm to grasp the object with high precision, it is very important to obtain the three-dimensional coordinates of the object [9]. After determining the holding object, the feature operation is carried out according to the obtained contour data. Since the shape of the selected cylindrical object in the image is a rectangle, the mass center of the object can be obtained by using the area center method. The goal of the area-barycentric method is to find the barycentric coordinates of a given region,

Given area C and area K , its center of gravity can be calculated by equation (6).

$$\bar{u} = \frac{\sum u}{K}, \bar{v} = \frac{\sum v}{K}, \bar{w} = \frac{\sum w}{K} \tag{6}$$

Formula (6) is calculated to obtain the corner coordinates and centroid coordinates of the target object under the binocular CCD camera coordinate system, but also need to be converted into the robot coordinate system data information, is the effective data for grasping and handling actions. As shown in Figure 4, the two spatial coordinate systems are workpiece coordinate system $O_\mu - U_\mu V_\mu W_\mu$ and system $O_\sigma - U_\sigma V_\sigma W_\sigma$. The coordinate origin between the two coordinate systems is inconsistent, and there are three translation parameters $\Delta U, \Delta V, \Delta W$. The axes are also not parallel to each other, and there are three rotation parameters $\delta_u, \delta_v, \delta_w$. The coordinates of the same point in two coordinate

systems are (U_μ, V_μ, W_μ) and $(U_\sigma, V_\sigma, W_\sigma)$ respectively. The two coordinate systems can be made consistent by translation and rotation transformation of coordinate axes, and the conversion relationship between coordinates is as follows:

$$\begin{bmatrix} U_\mu \\ V_\mu \\ W_\mu \end{bmatrix} = \eta C \begin{bmatrix} U_\sigma \\ V_\sigma \\ W_\sigma \end{bmatrix} + T \quad (7)$$

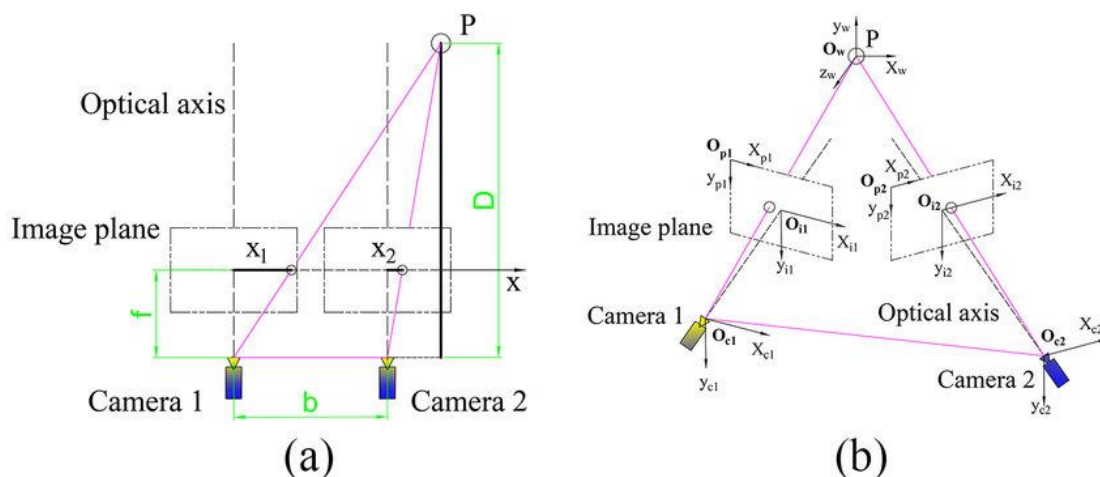


Figure 4. Conversion of binocular CCD camera coordinate system and robot coordinate system

The coordinate transformation method based on Rodrigue matrix is adopted here. η is the scale factor between the two coordinate systems. C is the rotation matrix. T is the translation matrix.

4. System Simulation

From the analysis of the intelligent baggage handling system at the airport, it can be seen that in this system, the role of lifting luggage is eight interwoven mechanical fingers, because the largest luggage on the market is 33 in. It will be a 33 in suitcase with a weight of 50 kg, as the largest grasp object that the manipulator can manipulate, to design the structure of the mechanical finger, the maximum size of the mechanical finger is designed to be 300 mm×40 mm×30 mm, and the load area is 200 mm×40 mm. This project takes 319 aluminum alloy as the main material, uses ANSYS software to establish its model, and constrains the hinge at the joint.

The deformation results are shown in Figure 5. In the process of stress, the deformation of the mechanical finger decreases from both ends to the hinged end in turn, with the maximum deformation of 0.03145mm and the minimum deformation of 0.001454mm. The deformation is very small, and it can be considered that the mechanical finger structure designed with this size belongs to the safe type. As can be seen from Figure 6, the area around the joint is subjected to the greatest stress, reaching 6.421 MPa. However, compared with this, the yield strength of aluminum alloy is 158.8 MPa, far exceeding the stress around the joint. From the deformation and force situation, the mechanical properties of the robot finger are very good, and it can lift 50 kilograms of luggage.

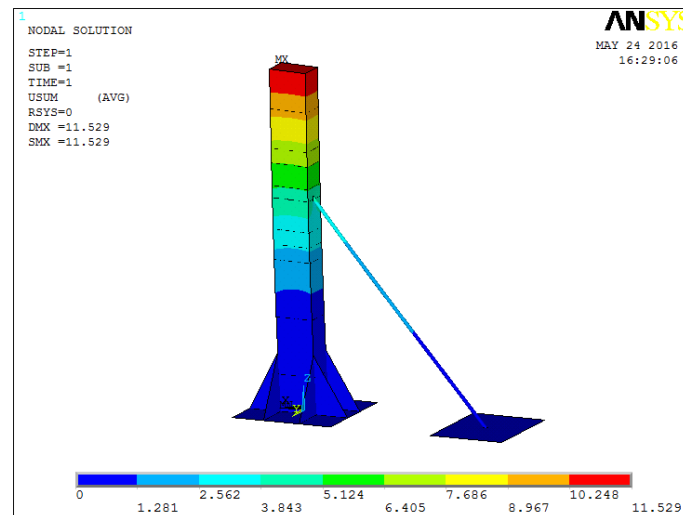


Figure 5. Deformation cloud image of mechanical parts

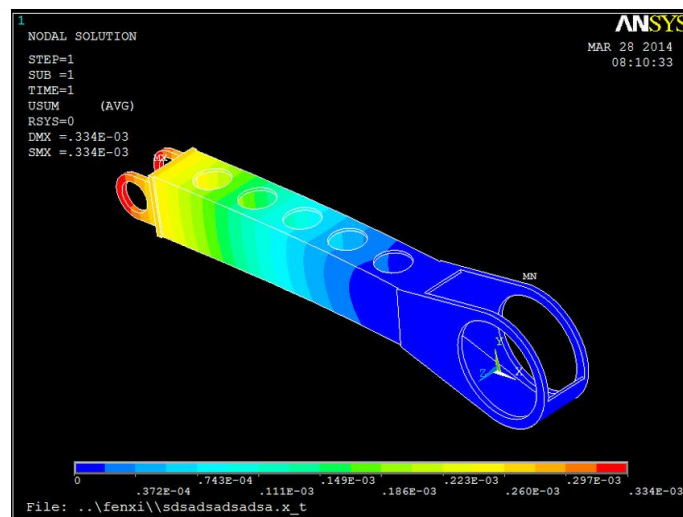


Figure 6. Stress nephogram of mechanical finger parts

5. Conclusion

The Freescale 16-bit MCU MC9S12DGI28 control processor is used to complete the automatic adjustment of the robot's speed and Angle. With NRF905 as the core, the data communication between host and host is completed. The method can be based on the data of airport baggage handling road and decision to achieve the visual location of the target. Solved the problem of inconvenient baggage handling at the airport.

References

- [1] Xiu Jiwei, Zhan Hongwei, Sun Jianwei, et al. Design of intelligent baggage handling system in airport. Journal of Mechanical Engineering, vol. 4, pp.136-138, April 2021.
- [2] Wu Haogang, YUAN Xulu, WANG Hui. Research on safety integrity of intelligent lifting and handling system. Lifting and Transportation Machinery, vol.7 , pp.28-31, July 2022.
- [3] Cui Yang, Wang Xue. Analysis and Optimization of cargo handling system in logistics enterprises. Journal of Jilin University of Chemical Technology, vol. 39, pp.69-74, September 2022.
- [4] Wu Xiyang. Research on intelligent baggage security check system based on Internet of Things and artificial intelligence technology. Computer Knowledge and Technology: Academic Edition, vol.17, pp.119-120, March 2021.

- [5] Zhang Rui, Sun Haoran, JIANG Yuanyuan. Research on intelligent storage system for material sorting and handling. *Research on Artificial Intelligence and Robotics*, vol.10, pp.110-115,February 2021.
- [6] Wu Ziyi, LAI Hongyu, Yang Pengqian, LIU Yidi. The utility model relates to a multi-UAV combined handling system for logistics. *Science and Technology Horizons*, vol. 8, pp.33-35, March 2022.
- [7] Li Tong. Design of garbage sorting system based on artificial intelligence robot arm. *Manufacturing and Upgrading Today*, vol. 4, pp.50-52, November 2022.
- [8] He Guangming, Shuai Jianghua. Design of multi-mode manipulator handling system based on PLC. *Technology & Market*, vol. 29, pp.70-72, November 2022.
- [9] Li Yanwen, Lou Peihuang, Lou Hangfei, et al. Research on McNamm wheel AGV motion control in cooperative handling system. *Machine Building and Automation*, vol.50, pp.224-227, June 2021.